Inorganic Chemistry
Article

Inorg. Chem. **2009**, *48*, 10811–10818 **10811**
DOI: 10.1021/ic901443x

Parametric Analysis of the Crystal Field Splitting Pattern of Sm(η^5-C_5Me_5)$_3$ Derived on the Basis of Absorption Spectra of Pellets or Solutions and Electronic Raman Spectra of Oriented Single Crystals†

Hanns-Dieter Amberger,*,‡ Hauke Reddmann,‡ and William J. Evans§

‡*Institut für Anorganische und Angewandte Chemie der Universität Hamburg, Martin-Luther-King-Platz 6, D-20146 Hamburg, Germany, and* §*Department of Chemistry, University of California, Irvine, California 92697-2025*

Received July 22, 2009

By comparing the absorption spectrum of pseudo trigonal planar Sm(η^5-C_5Me_5)$_3$ (**1**) (KBr pellet, methylcyclohexane solution) with the previously assigned one of Sm(η^5-C_5Me_4H)$_3$ (**2**) a truncated experimental crystal field (CF) splitting pattern of the former compound could be derived in the NIR range. Because of its dark brown color, fluorescence is not observed from complex **1**, and thus the CF splitting pattern in the low energy range could not be determined on the basis of luminescence measurements. However, comparing the FIR and MIR spectra (pellets) as well as the Raman spectra of oriented single crystals of **1** with those of La(η^5-C_5Me_5)$_3$ (**3**) at least two additional CF levels could be detected. The free parameters of a phenomenological Hamiltonian were fitted to the thus extended CF splitting pattern of **1**, leading to a reduced rms deviation of 15.0 cm^{-1} for 21 assignments. On the basis of these phenomenological CF parameters, the global CF strength experienced by the Sm^{3+} central ion was estimated, and seems to be the third largest one ever encountered in Sm^{III} chemistry. The obtained Slater parameter F^2 and the spin−orbit coupling parameter ζ_{4f} allow the insertion of compound **1** into empirical nephelauxetic and relativistic nephelauxetic series, respectively, of Sm^{III} compounds. With its low F^2 value, complex **1** is the most covalent Sm^{III} compound (considering only f electrons) found to date. The experimentally based non-relativistic molecular orbital scheme (in the f range) of complex **1** was set up and compared with the results of a previous Xα-SW calculation on the pseudo trigonal planar model compound Sm(η^5-C_5H_5)$_3$. In the frame of the search for f-f and electronic Raman transitions, the vibrational spectra (FIR/MIR of pellets, Raman spectra of oriented single crystals) of compound **1** were recorded too, and partly assigned on the basis of the observed coincidences and polarizations.

1. Introduction

In the case of air-stable and thus cut- and polishable solids, the symmetries of the crystal field (CF) states of an f element compound under consideration are usually derived in the UV/vis/NIR range from absorption (linear dichroism spectra,[1] LD) and in the FIR/MIR/NIR range from luminescence spectra (luminescence anisotropy[2]) of transparent α, σ and π oriented[3] single crystals.[4,5] However, dark colored compounds frequently do not fluoresce, and thus the missing CF levels in the low energy range have to be extracted from rare f-f transitions in the FIR/MIR spectra[4] or from even more rare electronic Raman transitions.[6]

Organometallic complexes of f elements are usually air-sensitive, have poor crystallizing properties, and are prone to phase transitions. In addition, the principal rotation axes of the individual molecules in the unit cell are frequently not aligned.[7−9] Even if they were aligned, as in the case of

† Part 71 of the series "Electronic Structures of Organometallic Compounds of f Elements". For part 70, see: Amberger, H.-D.; Reddmann, H. Z. Anorg. Allg. Chem. 2009, 635, 291.

*To whom correspondence should be addressed. E-mail: fc3a501@uni-hamburg.de.

(1) Rodger, A.; Nordèn, B. *Circular Dichroism and Linear Dichroism*; Oxford University Press: Oxford, 1997; and references therein.

(2) Feofilov, P. P. *The Physical Basis of Polarized Emission: Polarized Luminescence of Atoms, Molecules, and Crystals*; Fizmatgiz: Moscow, 1959; Consultants Bureau, New York, 1961; and references therein.

(3) Dieke, G. H. *Spectra and Energy Levels of Rare Earth Ions in Crystals*; Interscience Publishers: New York, 1968, p 126.

(4) Görller-Walrand, C.; Binnemans, K. Rationalization of Crystal Field Parametrization. In *Handbook on the Physics and Chemistry of Rare Earths*; Gschneidner, K. A., Jr., Eyring, L., Eds.; Elsevier Science B. V.: Amsterdam, 1996; Vol. *23*, Chapter 155; and references therein.

(5) Reid, M. F. Transition Intensities. In *Spectroscopic Properties of Rare Earths in Optical Materials*; Liu, G., Jacquier, B., Eds.; Springer-Verlag: Berlin, 2005; Chapter 2, p 98; and references therein.

(6) Koningstein, J. A.; Mortensen, O. S. Electronic Raman Transitions. In *The Raman Effect*; Anderson, A., Ed.; Dekker: New York, 1973; Vol. *2*, p 519; and references therein.

(7) Schumann, H.; Meese-Marktscheffel, J. A.; Esser L. *Chem. Rev*. **1995**, *95*, 865; and references therein.

(8) Bombieri, G.; Paolucci, G. Organometallic π Complexes of the f-Elements. In *Handbook on the Physics and Chemistry of Rare Earths*; Gschneidner, K. A., Jr., Eyring L., Eds.; Elsevier Science B. V.: Amsterdam, 1998; Vol. *25*, Chapter 168; and references therein.

(9) Amberger, H.-D.; Edelmann, F. T.; Gottfriedsen, J.; Herbst-Irmer, R.; Jank, S.; Kilimann, U.; Noltemeyer, M.; Reddmann, H.; Schäfer, M. *Inorg. Chem*. **2009**, *48*, 760.

Published on Web 10/16/2009

low-symmetric crystal systems,[10] it is difficult to orientate these rotation axes with respect to an external vector field. Thus, during the past decades the results of LD measurements of f element organometallics were only reported for the σ complexes $Ln\{CH(SiMe_3)_2\}_3$ (Ln = Nd,[11] Er[12]), and some base adducts of the $LnCp_3$ moiety (Ln = Pr,[13,14] Nd;[15] Cp = η^5-C_5H_5). Recent efforts to apply this method also to homoleptic pseudo (ψ) trigonal planar $LnCp'_3$ complexes were successful for $Ln(C_5Me_4H)_3$ (Ln = Pr,[16] Nd,[17,18] Sm[19]) but failed previously for $LnCp^*_3$ (Ln = Pr, Nd, Sm; Cp* = η^5-C_5Me_5), presumably because of single crystals of insufficient size. However, recently we succeeded in recording the σ and π luminescence spectra of small oriented single crystals of $LnCp^*_3$ (Ln = Pr, Nd) in a limited energy range using a Raman instrument (equipped with a microscope) applying the exciting lines at 532 and 785 nm, respectively.[20]

$LnCp^*_3$ and $Ln(C_5Me_4H)_3$ complexes have very similar molecular structures,[21−27] leading most probably to comparable electronic structures, and hence to closely related optical spectra. By comparing the absorption spectrum of $SmCp^*_3$ (**1**) with the recently assigned one (on the basis of LD measurements) of $Sm(C_5Me_4H)_3$ (**2**)[19] we can derive the corresponding truncated CF splitting pattern of **1** in the NIR range.

In the case of yellow or orange organometallic Sm^{III} complexes of the stoichiometries $[SmCp_3(X)]$ (X = CNC_6H_{11},[28] $NCCH_3$,[29] THF[30]), $[Cp_3La_{0.8}Sm_{0.2}(NCCH_3)_2]$[29], and $Sm(C_5H_4CH_2CH_2OCH_3)_3$[31] the CF splitting patterns in the low energy range could be extracted from the luminescence transitions $^4G_{5/2}\rightarrow{}^6H_J$ (J = 5/2, 7/2, 9/2, 11/2, 13/2). Dark Sm^{III} organometallics such as deep red $Sm(C_5H_4t\text{-}Bu)_3$,[30] red brown **2**[19] and dark brown **1** do not exhibit fluorescence and thus information about the CF splitting patterns in the low energy range is missing. However, by comparing the FIR/MIR spectra of pellets and the Raman spectra of oriented single crystals of $Ln(C_5Me_4H)_3$ (Ln = Ce, Pr, Sm) with those of $La(C_5Me_4H)_3$ we recently detected f-f transitions in the FIR/MIR spectra in the case of Ln = Ce,[32] Pr,[16] and electronic Raman transitions[6,33] in the case of Ln = Pr,[16] Sm.[34] For this reason, we hoped to find some additional low energetic CF levels of **1** by comparing the FIR/MIR spectra (pellets) and Raman spectra (oriented single crystals) of complex **1** with those of $LaCp^*_3$ (**3**).

In this report, the thus somewhat extended experimental CF splitting pattern is simulated by fitting the free parameters of a phenomenological Hamiltonian (see ref 4 (p 167)). From the parameters obtained, the Cp* ligand can be inserted into empiric spectrochemical, nephelauxetic, and relativistic nephelauxetic series of Sm^{III} compounds. Also, the experimentally based non-relativistic molecular orbital (MO) scheme (in the f range)[35] of **1** can be set up, and can be compared with the results of a previous Xα-SW calculation on the ψ trigonal planar model complex $Sm(\eta^5\text{-}C_5H_5)_3$.[36] In the frame of the search for f-f transitions in the FIR/MIR range and electronic Raman transitions, the vibrational FIR/MIR (pellets) and polarized Raman spectra of oriented single crystals were recorded too. The observed coincidences and polarizations allow some assignments of the skeletal vibrations.

2. Experimental Section

Small single crystals of dark brown $SmCp^*_3$ (**1**) and yellow $LaCp^*_3$ (**3**) were synthesized at the University of California, Irvine, adopting the more actual improved procedure of Evans et al.[37] The absorption spectra in the NIR (KBr pellets, methylcyclohexane solutions) and MIR (KBr pellets) as well as FIR (polyethylene pellets) ranges were recorded by means of Cary 5e (Varian) and Vertex 70 (Bruker) instruments, respectively. The former can be combined with a bath cryostat using liquid N_2 or liquid He as coolant. For running the Raman spectra (powdered material and single crystals sealed in glass tubes), the recently developed Senterra instrument (Bruker) equipped with a microscope and lasers with exciting lines at 785, 632.8, and 532 nm was available. First orienting measurements showed that dark brown compound **1** exhibits unacceptable Raman spectra using the laser line at 532 nm, and only satisfactorily resolved ones with the laser line at 632.8 nm. Applying the 785 nm line, skeletal and innerligand vibrations up to 700 cm^{-1} were well-defined, the innerligand vibrations in the range 700−1500 cm^{-1} only satisfactorily resolved, and the ν(CH) vibrations were scarcely detectable. Polarizers and analyzers were set to positions pa/pa, pa/pe = pe/pa (in the case of axially symmetric systems), and pe/pe, where pa and pe mean parallel and perpendicular to the macroscopic axis of the rod-like single crystals of **1** and **3**. At the present stage, the relative orientations of the (antiparallel directed) trigonal principal axes of the two $LnCp^*_3$ molecules per unit cell (see Figure 1a) to the rod axis are not known from X-ray analyses. A comparison of the polarizations of the vibrational Raman spectra of small oriented single crystals of $LnCp^*_3$ (Ln=La, Pr, Nd, Sm) with

(10) Schulz, H.; Schultze, H.; Link, M.; Amberger, H.-D. *J. Organomet. Chem.* **1992**, *440*, 139.
(11) Guttenberger, C.; Unrecht, B.; Reddmann, H.; Amberger, H.-D. *Inorg. Chim. Acta* **2003**, *348*, 165.
(12) Reddmann, H.; Guttenberger, C.; Amberger, H.-D. *J. Organomet. Chem.* **2000**, *602*, 65.
(13) Amberger, H.-D.; Schulz, H. *Spectrochim. Acta* **1991**, *47A*, 233.
(14) Amberger, H.-D.; Schulz, H. *J. Organomet. Chem.* **1993**, *443*, 71.
(15) Schulz, H.; Hagen, C.; Reddmann, H.; Amberger, H.-D. *Z. Anorg. Allg. Chem.* **2004**, *630*, 268.
(16) Amberger, H.-D.; Reddmann, H. *Z. Anorg. Allg. Chem.* **2008**, *634*, 1542.
(17) Amberger, H.-D.; Reddmann, H. *Z. Anorg. Allg. Chem.* **2006**, *632*, 1953.
(18) Amberger, H.-D.; Reddmann, H. *Z. Anorg. Allg. Chem.* **2007**, *633*, 443.
(19) Amberger, H.-D.; Reddmann, H. *J. Organomet. Chem.* **2009**, *635*, 291.
(20) Amberger, H.-D.; Reddmann, H.; Mueller, T. J.; Evans, W. J. *Inorg. Chem.*, submitted for publication.
(21) Evans, W. J.; Gonzales, S. L.; Ziller, J. W. *J. Am. Chem. Soc.* **1991**, *113*, 7423.
(22) Evans, W. J.; Seibel, G. A.; Ziller, J. W. *J. Am. Chem. Soc.* **1998**, *120*, 6745.
(23) Evans, W. J.; Perotti, J. M.; Kozimor, S. A.; Champagne, T. M.; Davis, B. L.; Nyce, G. W.; Fujimoto, C. H.; Clark, R. D.; Johnston, M. A.; Ziller, J. W. *Organometallics*. **2005**, *24*, 3916; and references therein.
(24) Evans, W. J.; Davis, B. L; Champagne, T. M.; Ziller, J. W. *Proc. Natl. Acad. Sci.* **2006**, *34*, 12678.
(25) Schumann, H.; Glanz, M.; Hemling, H. *J. Organomet. Chem.* **1993**, *445*, C1.
(26) Schumann, H.; Glanz, M.; Hemling, H.; Hahn, F. E. *Z. Anorg. Allg. Chem.* **1995**, *621*, 341.
(27) Evans, W. J.; Rego, D. B.; Ziller, J. W. *Inorg. Chem.* **2006**, *45*, 10790.
(28) Reddmann, H.; Schultze, H.; Amberger, H.-D.; Shalimoff, G. V.; Edelstein, N. M. *J. Alloys Compd.* **1992**, *180*, 337.
(29) Schulz, H.; Reddmann, H.; Amberger, H.-D. *J. Organomet. Chem.* **1993**, *461*, 69.
(30) Amberger, H.-D.; Reddmann, H.; Jank, S.; Lopes, M. I.; Marques, N. *Eur. J. Inorg. Chem.* **2004**, 98.
(31) Qian, C.; Wang, B.; Edelstein, N. M.; Reddmann, H.; Amberger, H.-D. *J. Alloys Compd.* **1994**, *207-208*, 87.
(32) Amberger, H.-D.; Reddmann, H. *Z. Anorg. Allg. Chem.* **2008**, *634*, 173.
(33) Gächter, B. F. *J. Mol. Spectrosc.* **1976**, *63*, 1; and references therein.
(34) Amberger, H.-D.; Reddmann H., unpublished results.
(35) Jank, S.; Amberger, H.-D. *Acta Phys. Pol.* **1996**, *A 90*, 21.
(36) Strittmatter, R. J.; Bursten, B. E. *J. Am. Chem. Soc.* **1991**, *113*, 552.
(37) Evans, W. J.; Forrestal, K. J.; Leman, J. T.; Ziller, J. W. *Organometallics* **1996**, *15*, 527.

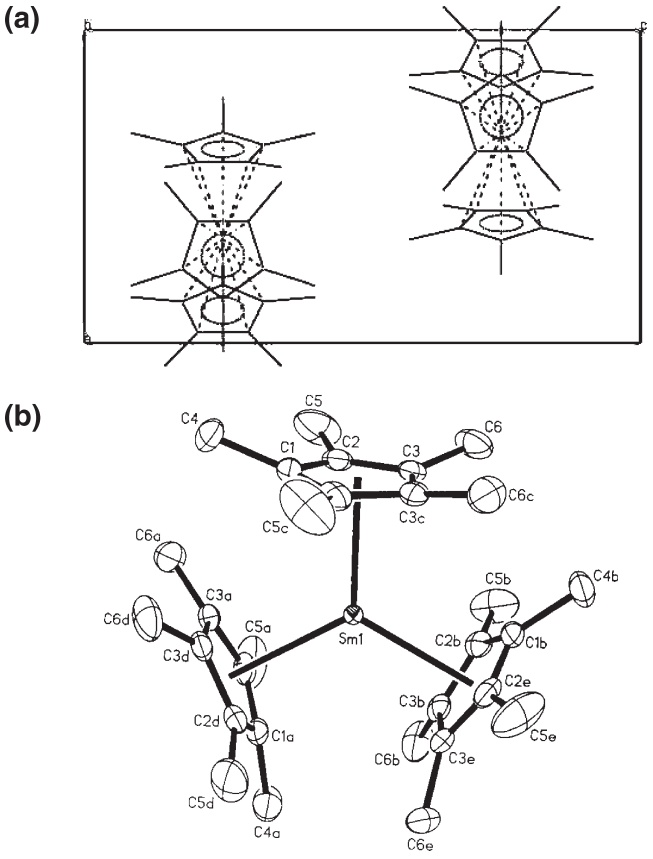

Figure 1. Structures of $SmCp^*_3$: (a) Crystal structure; (b) Molecular structure in the crystal, from ref 21.

those of $Ln(C_5Me_4H)_3$ (Ln = La,[34] Pr,[16] Nd,[18] Sm[34]) shows close relationships. The same holds also for the polarized luminescence spectra of $LnCp^*_3$[20] (Ln = Pr, Nd) and $Ln(C_5Me_4H)_3$ (Ln = Pr,[16] Nd[18]). In case of the latter class of compounds, the 3-fold axes are parallel to the rod axes. Thus, we assume that this also holds for $LnCp^*_3$.

3. Results and Discussion

3.1. Phenomenological Hamiltonian. The energy levels within f^n configuration in D_{3h} symmetry can be written in terms of the atomic free ion (H_{FI}) and CF (H_{CF}) Hamiltonians as follows:

$H = H_{FI} + H_{CF}$, where

$$H_{FI} = \sum_{k=0,2,4,6} f_k F^k(nf,nf) + a_{SO}\zeta_{4f} + \alpha L(L+1) + \beta G(G_2) + \gamma G(R_7) + \sum_{i=2,3,4,6,7,8} t_i T^i + \sum_{k=0,2,4} m_k M^k + \sum_{k=2,4,6} p_k P^k$$

(see ref 4 (p 167)) and

$$H_{CF}(D_{3h}) = B^2_0 C^{(2)}_0 + B^4_0 C^{(4)}_0 + B^6_0 C^{(6)}_0 + B^6_6 (C^{(6)}_{-6} + C^{(6)}_6)$$

(see ref 4 (p 242)).

The F^k(nf,nf)s and ζ_{4f} represent, respectively, the radial parts of the electrostatic and spin−orbit interactions between f electrons, while f_k and a_{so} are the angular parts of these interactions. α, β, and γ are the parameters associated with the two-body effective operators of configuration interaction, $G(G_2)$ and $G(R_7)$ being the Casimir operators of the groups G_2 and R_7, and L the orbital angular momentum. The T^is are the radial parts of the corresponding three-body effective operators t_iT^i. The M^k parameters represent the spin−spin, and spin−other−orbit interactions, while the P^k parameters arise from electrostatic spin−orbit interactions with higher configurations, with m_k and p_k being the corresponding operators. The CF interaction for the above symmetries is represented by the B^k_q parameters and the tensor operators $C^{(k)}_q$ (see ref 4 (p 170)).

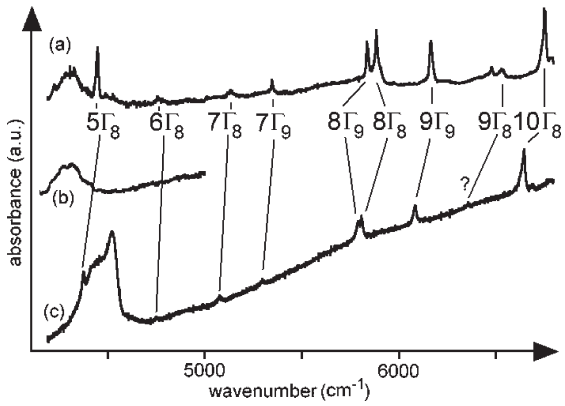

Figure 2. Absorption spectra of $LnCp'_3$ in the range 4000−6700 cm^{-1}: (a) Ln = Sm, Cp′ = C_5Me_4H (KBr pellet, ca. 77 K); (b) Ln = La, Cp′ = Cp* (KBr pellet, ca. 77 K) (c) Ln = Sm, Cp′ = Cp* (KBr pellet, room temperature).

3.2. Experimentally Derived CF Splitting Pattern of $SmCp^*_3$. The UV/vis/NIR spectra of compound **1** were run as KBr pellets and solutions in methylcyclohexane at room temperature and about 77 K. Because of a low-lying charge transfer band, f-f transitions could be observed only up to about 11400 cm^{-1}. Apart from signals due to the solvent (especially in the range 5300−5700 cm^{-1}) the room temperature absorption spectra of the pellet and the solution are identical within experimental error, but the latter was better resolved. The low temperature spectra have the same appearance (however, with a poorer signal-to-noise ratio, and the band maxima shifted to higher energies by approximately 10 cm^{-1}), thus indicating an energetically isolated CF ground state. Because of these reasons, room temperature spectra of **1** are shown in Figures 2−4, and in the energy range 4200−6700 cm^{-1} covered by Figure 2, the pellet spectrum is preferred to the solution spectrum.

The close resemblance of the absorption spectrum of compound **1** in the NIR range with the recently assigned one of **2**[19] (see Figures 2−4) allowed to derive a widely secured truncated experimental CF splitting pattern of **1** between 4350 and 11400 cm^{-1} (see Table 1). Only the assignment of some weaker signals (marked with "?") which might be possibly due to vibronic or (in principle) symmetry forbidden transitions of $\Gamma_7 \rightarrow \Gamma_7$ type (see ref 4 (p 255)) is somewhat doubtful.

The f-f transitions of **1** have lower energies than the corresponding ones of **2**, thus indicating somewhat lower electronic repulsion and spin−orbit coupling parameters of f electrons for **1**.

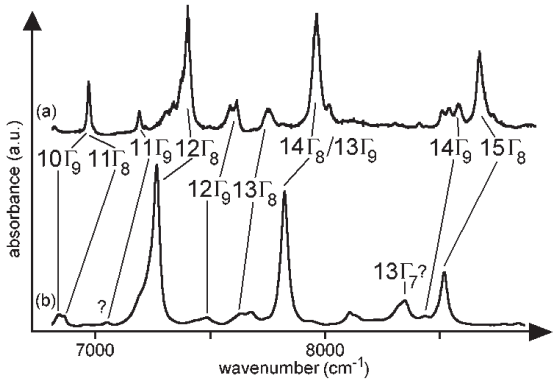

Figure 3. Absorption spectra of $SmCp'_3$ in the range 6800−8900 cm^{-1}: (a) Cp′=C_5Me_4H (KBr pellet, ca. 77 K); (b) Cp′=Cp* (methylcyclohexane solution, room temperature).

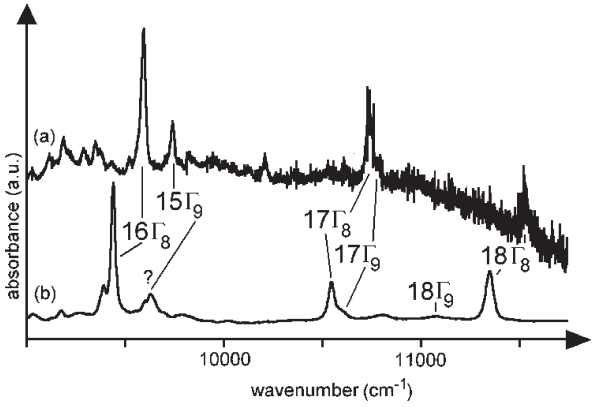

Figure 4. Absorption spectra of $SmCp'_3$ in the range 9000−11700 cm^{-1}: (a) Cp′=C_5Me_4H (KBr pellet, ca. 77 K); (b) Cp′=Cp* (methylcyclohexane solution, room temperature).

Using the exciting line at 632.8 nm, powdered material or oriented single crystals of complex **1** exhibit Raman signals at 486 (weak), 920 (strong), and 2631 cm^{-1} (medium), which are not present in the Raman spectrum of **3**, and thus might be of electronic origin. The intensity ratio of electronic and vibrational Raman peaks decreases with the wavelength of the exciting line. In Figure 5, the electronic nature of the strong band at 920 cm^{-1} is proved by the finding that the intensity of this signal decreases going from the exciting line at 632.8 nm to that 785 nm, if the intensity of the triplet of vibrations around 600 cm^{-1} is kept constant. The same holds for the weak signal at 486 cm^{-1}. The remaining band at 2631 cm^{-1} could not be detected using the exciting line at 785 nm, presumably because of the insensitivity of the CCD detector at approximately 10000 cm^{-1} (absolute wavenumbers).

From the electronic Raman transitions at 486, 920, and 2631 (?) cm^{-1} only the first has a clear counterpart in the FIR/IR spectrum (see Figure 6), the second corresponds only to a shoulder (which is missing in the case of **3**) and the third could not be detected.

Considering the usually slight lowering of the energies of the corresponding CF levels of **1** compared to **2** (vide supra), the levels with experimental energies of 486, 920 (and possibly also 2631 cm^{-1}) of **1** have to be correlated with the calculated CF energies of complex **2** of 556, 914, and 2750 cm^{-1} of the levels $1\Gamma_9(^6H_{5/2})$, $2\Gamma_7(^6H_{7/2})$, and $4\Gamma_7(^6H_{9/2})$.[19]

Table 1. Calculated and Experimental Energy Levels (in cm^{-1}) for $SmCp^*_3$

multiplet	CF level		E (calc.)	E (exp.)	ΔE
$^6H_{5/2}$ [a]	$1\Gamma_7$ [b]	±5/2 [c]	0	0	0
$^6H_{5/2}$	$1\Gamma_9$	±3/2	507	486	21
$^6H_{7/2}$	$2\Gamma_7$	±7/2	910	920	−10
$^6H_{5/2}$	$1\Gamma_8$	±1/2	948		
$^6H_{7/2}$	$3\Gamma_7$	±5/2	1617		
$^6H_{7/2}$	$2\Gamma_9$	±3/2	1886		
$^6H_{7/2}$	$2\Gamma_8$	±1/2	1921		
$^6H_{9/2}$	$3\Gamma_9$	±9/2	2498		
$^6H_{9/2}$	$4\Gamma_7$	±7/2	2666	(2631) [d,e]	(35)
$^6H_{9/2}$	$3\Gamma_8$	±1/2	2967	(2965) [e]	(2)
$^6H_{9/2}$	$4\Gamma_9$	±3/2	3073		
$^6H_{9/2}$	$5\Gamma_7$	±5/2	3103		
$^6H_{11/2}$	$4\Gamma_8$	±11/2	3585		
$^6H_{11/2}$	$5\Gamma_9$	±9/2	3806		
$^6H_{11/2}$	$6\Gamma_7$	±7/2	4123		
$^6H_{11/2}$	$5\Gamma_8$	±1/2	4369	4376	−7
$^6H_{11/2}$	$6\Gamma_9$	±3/2	4442		
$^6H_{11/2}$	$7\Gamma_7$	±5/2	4545		
$^6H_{13/2}$	$6\Gamma_8$	±13/2	4748	4751	−3
$^6H_{13/2}$	$7\Gamma_8$	±11/2	5049	5074	−25
$^6H_{13/2}$	$7\Gamma_9$	±9/2	5281	5297	−16
$^6H_{13/2}$	$8\Gamma_7$	±7/2	5337		
$^6H_{15/2}$	$8\Gamma_9$	±15/2	5787	5788	−1
$^6H_{13/2}$	$8\Gamma_8$	±1/2	5823	5808	15
$^6H_{13/2}$	$9\Gamma_7$	±5/2	6017		
$^6H_{13/2}$	$9\Gamma_9$	±3/2	6103	6083	20
$^6H_{15/2}$	$9\Gamma_8$	±13/2	6440	(6357)	(83)
$^6H_{15/2}$	$10\Gamma_8$	±11/2	6653	6642	11
$^6H_{15/2}$	$10\Gamma_9$	±9/2	6842	6844	−2
$^6F_{1/2}$	$11\Gamma_8$	±1/2	6892	6868	24
$^6H_{15/2}$	$11\Gamma_7$	±7/2	7084		
$^6F_{3/2}$	$11\Gamma_9$	±3/2	7114	(7053)	(61)
$^6F_{3/2}$	$12\Gamma_8$	±1/2	7264	7262	2
$^6H_{15/2}$	$11\Gamma_7$	±5/2	7394		
$^6H_{15/2}$	$12\Gamma_9$	±3/2	7482	7485	−3
$^6F_{5/2}$	$12\Gamma_7$	±5/2	7581		
$^6H_{15/2}$	$13\Gamma_8$	±1/2	7622	7632	−10
$^6F_{5/2}$	$14\Gamma_8$	±1/2	7809	7822	−13
$^6F_{5/2}$	$13\Gamma_9$	±3/2	7830	7822	8
$^6F_{7/2}$	$13\Gamma_7$	±7/2	8372	(8347)	(25)
$^6F_{7/2}$	$14\Gamma_9$	±3/2	8440	8433	7
$^6F_{7/2}$	$15\Gamma_8$	±1/2	8500	8519	−19
$^6F_{7/2}$	$14\Gamma_7$	±5/2	8523		
$^6F_{9/2}$	$16\Gamma_8$	±1/2	9436	9443	−7

[a] Dominating Russell−Saunders multiplet $^{2S+1}L_J$. [b] The Bethe Γ notation for the double group D'_{3h} is used. The irreps Γ_i are ordered in ascending energy. [c] Largest eigenvector component ± M_J. [d] Energies in parentheses were not used in the fit. [e] See text.

A closer inspection of the MIR spectra of complexes **1** and **3** in most regions exhibits no significant differences, but **1** in the range of ν(CH) vibrations shows a strong triplet at 2855, 2913, and 2965 cm^{-1} of comparable transmittance, whereas the latter signal has a considerably higher transmittance in the case of **3** and other $LnCp^*_3$ (Ln = Ce, Pr, Nd) compounds.[20] This finding suggests the coincidence of a ν(CH) vibration and an f-f transition at 2965 cm^{-1}. The corresponding Raman spectrum of **1** (laser line at 632.8 nm) is comparable with that of **3**, hence a CF level at 2965 cm^{-1} is highly probable but not definitely proven.

The free parameters of the above-mentioned phenomenological Hamiltonian of the f^5 configuration (see ref 4 (p 167)) were fitted to the energies of the reliably assigned CF levels. Neither the assigned CF states with energies higher than 9600 cm^{-1} (which have strong deviations between calculated and experimental values in the case of **2**[19] and $Sm(C_5H_4t\text{-}Bu)_3$,[30] presumably because of an

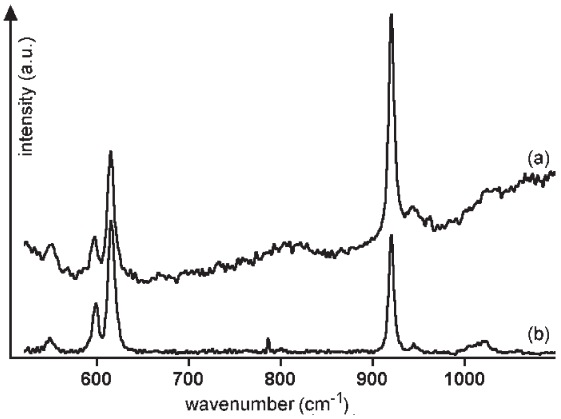

Figure 5. Raman spectrum of an oriented single crystal of $SmCp^*_3$ (polarizer/analyzer combination pe/pe) in the range 450−1100 cm^{-1}: (a) exciting line at 632.8 nm; (b) exciting line at 785 nm.

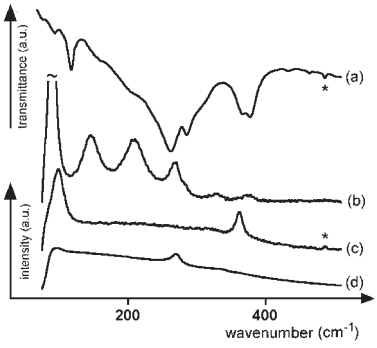

Figure 6. Vibrational spectra of $SmCp^*_3$ in the range 80−500 cm^{-1}: (a) FIR spectrum (polyethylene pellet); (b) Raman spectrum (oriented single crystal, exciting line at 785 nm, polarizer/analyzer combination pe/pe; (c) as (b), pa/pe; (d) as (b), pa/pa. The stars indicate an f-f transition in the FIR and an electronic Raman transition in the Raman spectrum.

adjacent charge-transfer band) nor the not definitively proven states at 2631 and 2965 cm^{-1} (vide supra) were considered in this calculation (see Table 1).

As a starting parameter set for the free ion and the CF parameters B^k_q, those of **2** were chosen. After some fitting cycles (only the Slater, spin−orbit coupling, and the CF parameters were varied), a reduced rms deviation (see ref 4 (p 164)) of 15.0 cm^{-1} was achieved for 21 assignments (see Tables 1, 2).

The parameter $N_v/(4\pi)^{1/2}=[\sum_{k,q}(B^k_q)^2/(2k+1)]^{1/2}$ is considered as a relative measure of the CF strength experienced by the central Ln^{3+} ion.[39] Inserting the CF parameters of **1** into the above-mentioned relation, one ends up with an $N_v/(4\pi)^{1/2}$ value of 1717 cm^{-1} (see Table 2). In Table 3, this value is compared to those of other Sm^{III} compounds. Obviously, the central ion of complex **1** experiences the third-highest CF strength found to date for Sm^{III} compounds. Those of homoleptic $Sm(C_5Me_4H)_3$[19] and $Sm(C_5H_4t\text{-}Bu)_3$[30] are somewhat larger, but those of the mono adducts $[SmCp_3(NCCH_3)]$,[29] $[SmCp_3(CNC_6H_{11})]$,[28] $[SmCp_3(THF)]$[30] and especially of the bis base adducts $[La_{0.8}Sm_{0.2}(Cp)_3(NCCH_3)_2]$[29] or $Sm(C_5H_4CH_2CH_2OCH_3)_3$[31] are considerably lower (see Table 3). This finding may be explained by the shorter Sm−C distances of **2** (276 pm) and the larger Sm−C distances of the bis and mono adducts compared to **1** (282 pm). Furthermore, according to the results of model calculations, the addition of one and, even more, of two axial ligands considerably reduces (assuming constant Ln−C bond lengths) the absolute value of the dominant CF parameter B^2_0,[35,40] leading to lower $N_v/(4\pi)^{1/2}$ values.

Table 2. Parameter Values (in cm^{-1}) for ψ Trigonal Planar $SmCp^*_3$, $Sm(C_5Me_4H)_3$, and $Sm(C_5H_4t\text{-}Bu)_3$

parameter	$SmCp^*_3$	$Sm(C_5Me_4H)_3$[a]	$Sm(C_5H_4t\text{-}Bu)_3$[b]
F^2	71817	72824	73992
F^4	56751	57547	58470
F^6	36292	36801	37391
ζ_{4f}	1129	1130	1143
α	[21.6] [c]	[21.6]	[21.6]
β	[−724]	[−724]	[−724]
γ	[1700]	[1700]	[1700]
T^2	[291]	[291]	[291]
T^3	[13]	[13]	[13]
T^4	[34]	[34]	[34]
T^6	[−193]	[−193]	[−193]
T^7	[288]	[288]	[288]
T^8	[330]	[330]	[330]
M^0	[2.4]	[2.4]	[2.4]
M^2	[1.34]	[1.34]	[1.34]
M^4	[0.91]	[0.91]	[0.91]
P^2	[341]	[341]	[341]
P^4	[256]	[256]	[256]
P^6	[171]	[171]	[171]
B^2_0	−2741	−2971	−2809
B^4_0	1341	1304	1483
B^6_0	1556	1433	1278
B^6_6	−2626	−2765	−2685
$N_v/(4\pi)^{1/2}$	1717	1814	1749
σ	15.0 (21) [d]	19.1 (19)	17.5 (25)

[a] From ref 19. [b] From ref 30. [c] Values in brackets held fixed on the values of $LaCl_3:Sm^{3+}$.[38] [d] Number of fitted energies in parentheses.

Table 3. Comparison of the F^2, ζ_{4f}, and $N_v/(4\pi)^{1/2}$ Values (in cm^{-1}) of $SmCp^*_3$ with Those of Selected Sm^{III} Compounds

compound[a]	F^2	ζ_{4f}	$N_v/(4\pi)^{1/2}$	ref
$LaF_3:Sm^{3+}$	79805	1176	610	41
$[Na_3\{Sm(ODA)_3\}\cdot 2NaClO_4\cdot 6H_2O]$[b]	79015	1166	755	42
$SmTp_3$[c]	78467	1169	487	43
$Sm(Cp)(Tp^{Me}2)_2$[d]	78293	1159	522	30
$GdOCl:Sm^{3+}$	78196	1150	640	44
$LaCl_3:Sm^{3+}$	78125	1168	300	38
$Cs_2NaSmCl_6$	77510	1167	545	45
$[La_{0.8}Sm_{0.2}(Cp)_3(NCCH_3)_2]$	77002	1155	1222	29
$[Sm\{N(SiMe_3)_2\}_3(CNC_6H_{11})_2]$	76676	1169	891	46
$Sm(C_5H_4CH_2CH_2OCH_3)_3$	76602	1156	1198	30
$Sm\{N(SiMe_3)_2\}_3$	76388	1164	1179	47
$[Sm(C_5H_4SiEt_3)_3(NCCH_3)]$	76305	1149	1375	48
$[SmCp_3(NCCH_3)]$	76230	1148	1324	29
$[SmCp_3(CNC_6H_{11})]$	75813	1151	1373	28
$[SmCp_3(THF)]$	75773	1149	1378	31
$[Sm(C_5H_4t\text{-}Bu)_3(THF)]$	75324	1149	1371	31
$Sm(C_5H_4t\text{-}Bu)_3$	73992	1143	1749	31
$Sm(C_5Me_4H)_3$	72824	1130	1813	19
$SmCp^*_3$	71817	1129	1717	this paper

[a] Ordered by decreasing Slater parameter F^2. [b] ODA = oxidiacetato. [c] Tp = hydrotris(pyrazolyl)borato. [d] $Tp^{Me}2$ = hydrotris(3,5-dimethylpyrazolyl)borato.

(38) Carnall, W. T.; Crosswhite, H.; Crosswhite, H. M. *Energy Level Structure and Transition Probabilities in the Spectra of the Trivalent Lanthanides in LaF_3*; ANL Report: 1977, unpublished; Appendix I, Table 1.
(39) Auzel, F.; Malta, O. L. *J. Phys.* (*Paris*) **1983**, *44*, 201.
(40) Apostolidis, C.; Kanellakopulos, B.; Klenze, R.; Reddmann, H.; Schulz, H.; Amberger, H.-D. *J. Organomet. Chem.* **1992**, *426*, 307.

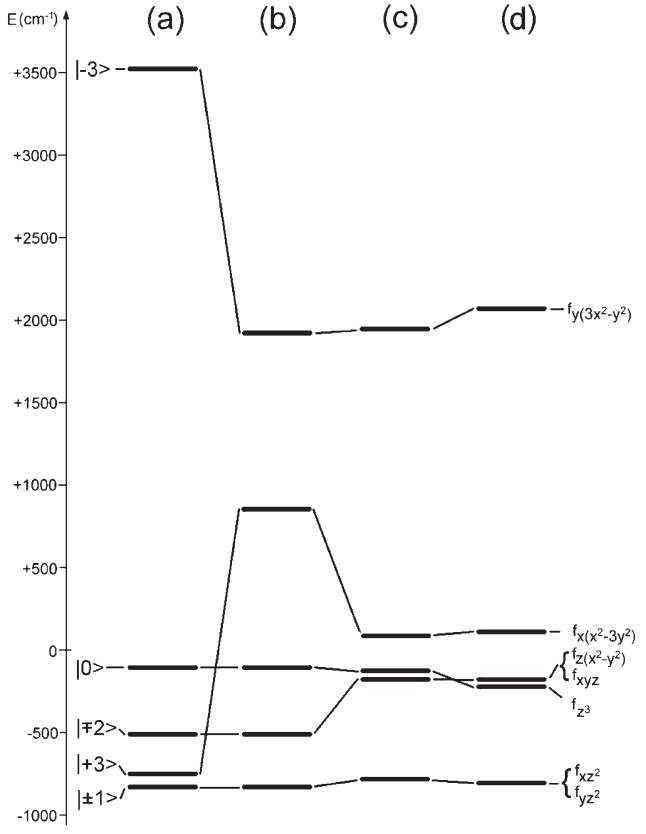

Figure 7. Experimentally based and calculated non-relativistic MO schemes of: (a) ψ trigonal planar Sm(η^5-Cp)$_3$ (calc., from ref 37); (b) like (a), but B_6^6 reduced to a quarter; (c) SmCp*$_3$, experimentally based; (d) Sm(C_5Me_4H)$_3$, experimentally based (from ref 19).

Obviously, complex **1** has the lowest F^2 value of all Sm^{III} compounds analyzed hitherto (see Table 3), and thus is the most covalent[49] compound (considering only f orbitals).

The eigenvalues of an energy matrix of the spin-free f^1 system, into which the CF parameters of a previous parametric analysis of the compound of interest had been inserted, were defined as the experimentally based non-relativistic MO scheme of this compound in the f range.[35]

In Figure 7, the experimentally based non-relativistic MO schemes (in the f range) of complexes **1** and **2** are compared with the non-relativistic MO scheme of the ψ trigonal planar model complex Sm(η^5-C_5H_5)$_3$ calculated in the framework of the Xα-SW approximation.[36] Obviously, the calculated total splitting of f orbitals is considerably greater than the experimentally based one.

Table 4. Selection Rules for IR (Pellet) and Raman (Powder) As Well As Polarized Raman Spectra Assuming Local D_{3h} (Skeletal Modes) and C_{5v} (Innerligand Modes) Symmetry, Respectively, of ψ Trigonal Planar LnCp*$_3$ Complexes (below 400 cm^{-1})

		FIR	Raman			
		pellet	powder	pa/pa	pa/pe	pe/pe
n[a]	D_{3h}					
1	A_1'	−	+	+	−	+
1	A_1''	−	−	−	−	−
1	A_2'	−	−	−	−	−
2	A_2''	+	−	−	−	−
3	E′	+	+	−	−	+
2	E″	−	+	−	+	−
	C_{5v}					
1	a_1	+	+	+	−	+
2	e_1	+	+	−	+	−
2	e_2	−	+	−	−	+

[a] Numbers of irreducible representations of excited vibrational levels.

Fitting the free parameters of the phenomenological Hamiltonian of the spin-free f^1 system to the calculated energies of f orbitals of Sm(η^5-C_5H_5)$_3$ one arrives at $B_0^2 = -3443$ cm^{-1}, $B_0^4 = 2817$ cm^{-1}, $B_0^6 = 1296$ cm^{-1}, and $B_6^6 = -6033$ cm^{-1}.[30] Comparing these values with those of compound **1** (see Table 2), it becomes evident that first of all the CF parameters B_6^6 (which considers the interactions between orbitals $f_{x(x^2-3y^2)}$ and $f_{y(3x^2-y^2)}$ within the framework of CF theory) but also B_0^4 are heavily overestimated by the model calculation. To roughly reproduce the correct total splitting of f orbitals, B_6^6 has to be reduced to a quarter, giving also a correct sequence of levels (see Figure 7).

3.3. Vibrational Spectroscopy. In the frame of our activities to detect f-f transitions in the FIR/IR spectra of pellets and electronic effects in the Raman spectra of oriented single crystals of complex **1**, the corresponding vibrational spectra were recorded, too.

In principle, $3N - 6 = 222$ (with number of atoms $N = 76$) normal vibrations are expected for ψ-trigonal planar LnCp*$_3$ complexes. However, if one assumes local D_{3h} symmetry for the central ion and local C_{5v} symmetry for the Cp* ligand, the above-mentioned large number is reduced to 15 skeletal (A_1', A_1'', A_2', $2A_2''$, 3E′, 2E″)[50] and 24 innerligand vibrations ($3a_1$, a_2, $4e_1$, $6e_2$)[51] (for a better discrimination, the irreducible representations of the skeletal vibrations are written in caps, but the innerligand ones in lower case).

Considering, at first, the more interesting skeletal vibrations, transitions to the two excited vibrational levels of A_2'' and the three of E′ symmetry are allowed in the IR spectrum by the selection rules, and those to the single of A_1', the three of E′, and the two of E″ symmetry are allowed in the Raman spectrum (see Table 4),[50] thus leading to five signals in the IR and six in the Raman spectrum, with three coincidences of E′ symmetry.

However, this at first glance not too complicated looking situation becomes more complex as the out-of-plane bending modes (γCCH_3) of a_1 (IR, Raman allowed), e_1 (IR, Raman), and e_2 (Raman) symmetry as well as the

(41) Carnall, W. T.; Goodman, G. L.; Rajnak, K.; Rana, R. S. *J. Chem. Phys.* **1989**, *90*, 3443.
(42) May, S.; Reid, M. F.; Richardson, F. S. *Mol. Phys.* **1987**, *62*, 341.
(43) Reddmann, H.; Apostolidis, C.; Walter, O.; Rebizant, J.; Amberger, H.-D. *Z. Anorg. Allg. Chem.* **2005**, *631*, 1487.
(44) Hölsä, J.; Lamminmäki, R.-J. *J. Lumin.* **1996**, *69*, 311.
(45) Richardson, F. S.; Reid, M. F.; Dallara, J. J.; Smith, R. D. *J. Chem. Phys.* **1985**, *83*, 3813.
(46) Jank, S.; Ph.D. Thesis, Universität Hamburg, Hamburg, Germany, **1998**.
(47) Reddmann, H.; Jank, S.; Amberger, H.-D. *Spectrochim. Acta Part A* *53* **1997**, 495.
(48) Sievers, M.; Ph.D. Thesis, Universität Hamburg, Hamburg, Germany, **1998**.
(49) Tandon, S. P.; Mehta, P. C. *J. Chem. Phys.* **1970**, *52*, 5417.
(50) Aleksanyan, V. T.; Borisov, G. K.; Garbuzova, I. A.; Devyatykh, G. G. *J. Organomet. Chem.* **1977**, *131*, 251.
(51) Bencze, É.; Lokshin, B. V.; Mink, J.; Herrmann, W. A.; Kühn, F. E. *J. Organomet. Chem.* **2001**, *627*, 55.

Table 5. Comparison of Experimental and Calculated Energies (in cm^{-1}) of Selected Innerligand (Sorted by the Corresponding Values of NaCp*) As Well As Skeletal Vibrations of Various Cp* Compounds (below 400 cm^{-1})

	γ(C−C*)	γ(C−C*)	γ(C−C*)	β(C−C*)	β(C−C*)	ν(M−ring)	ν(M−ring)	ref
compound	a_1 IR/Ra	e_1 IR/Ra	e_2 Ra	e_2 Ra	e_1 IR/Ra	ν_s	ν_{as}	
NaCp* exp.	174	187	237	270	277	318	255	51
NaCp* NCA	175	187	230	261	270			51
NaCp* BLYP	149	250	137	261	266			51
$Cp^*Mn(CO)_3$ exp.	205	145	109	205	210	392	286	52
$Cp^*Mn(CO)_3$ NCA	201	153	113	201	214	388	286	52
$Cp^*Re(CO)_3$ exp.	173	173	104	173	190	381	280	52
$Cp^*Re(CO)_3$ NCA	173	172	108	173	188	374	280	52
Cp^*ReO_3 exp.	183	122	109	183	205	355	340	52
Cp^*ReO_3 NCA	179	122	109	179	205	353	340	52

Table 6. Observed Peak Energies (in cm^{-1}) in the Range below 400 cm^{-1} in the FIR (Pellet) and Raman Spectra (Powder, Polarized Spectra of Oriented Single Crystals) of $SmCp^*_3$

FIR	Raman			
pellet	powder	pa/pa	pa/pe	pe/pe
75 vw				
94 w	∼95 vs	∼96 vw	∼99 vs	∼93 vs
118 s				
	145 m			145 s
∼160 sh				
∼210 sh	210 m			210 s
263 vs				
	270 m	270 m		270 s
286 s	∼286 sh			∼286 sh
∼315 sh				
	330 br	330 vw		∼330 br
	362 m	360 vw	362 m	
367 s				
378 s	378 w			378 w

in-plane bending modes (βCCH_3) of e_1 (IR, Raman) and e_2 (Raman) symmetry of the Cp* ligand have comparable energies as the skeletal vibrations[51] (see Table 5). Thus, in the range below 400 cm^{-1} 8 signals are expected in the FIR and 11 in the Raman spectrum with 7 coincidences (see Table 4).

The wavenumbers of the observed signals in the FIR (see Figure 6a) and Raman spectra of powdered $SmCp^*_3$ are given in Table 6. Obviously, the observed numbers of clearly visible lines in the FIR and Raman spectra as well those of the coincidences are lower than the expected ones, thus complicating the assignment of the signals.

To possibly separate skeletal and innerligand vibrations, the currently available experimental and calculated data of selected (wavenumbers lower than 400 cm^{-1}) innerligand vibrations of Cp* compounds are summarized in Table 5. It can be seen from this table that the experimental values of the three γCCH_3 modes astonishingly move between 174 and 205, 122−187, 104−237, and those of the two βCCH_3 modes between 173 and 270 and 190−277 cm^{-1}, thus not allowing a reliable separation of skeletal and innerligand vibration of $SmCp^*_3$.

In the range below 400 cm^{-1} five stronger distinct bands at 378, 367, 286, 263, and 118 cm^{-1} appear in the FIR spectrum of a pellet (see Figure 6). Those at 378 and 286 cm^{-1} have counterparts in the Raman spectrum of powdered **1** (378, 286 cm^{-1}) but not that at 118 cm^{-1} (see Table 6). According to the selection rules of Table 4, the two former signals correspond to skeletal vibrations of E′, or innerligand vibrations of a_1 or e_1 symmetry, and the latter to a skeletal vibration of A_2'' symmetry, provided the selection rules of local D_{3h} and C_{5v} symmetry hold strictly. In case of the intense FIR signals at 367 and 263 cm^{-1} the situation is unsure, as the closest Raman bands at 362 and 270 cm^{-1} are off by 5 and 7 cm^{-1}, respectively (see Table 5). If coincidences do not take place, the FIR signals would correspond to skeletal vibrations of A_2'' symmetry (see Table 4).

Out of the distinct Raman signals at 210 and 145 cm^{-1} as well as the broad one at about 330 cm^{-1}, only the first and last of these signals correspond to diffuse shoulders in the FIR spectrum which allow no additional assignments.

However, this poor situation is somewhat improved by applying the much more detailed selection rules for polarized Raman transitions of oriented single crystals (see Table 4) to the corresponding experimental data of complex **1** (see Figure 6). The above-mentioned questionable Raman band at 270 cm^{-1} of powdered **1** appears in the Raman spectra of the pa/pa and pe/pe combinations of polarizer and analyzer (see Figure 6). According to the selection rules of Table 4, these polarization properties have to be correlated with a skeletal vibration of A_1', or an innerligand vibration of a_1 symmetry. Going through Table 5, innerligand vibrations of a_1 symmetry have wavenumbers far from 270 cm^{-1}, supporting the former assignment. The likewise questionable Raman band at 362 cm^{-1} of powdered **1** has only a counterpart in the polarized Raman spectrum of the pa/pe combination (see Figure 6), which suggests the correlation with a skeletal vibration of E″ or the innerligand mode of e_1 symmetry. An inspection of Table 5 excludes the latter alternative. The above-mentioned distinct Raman signals at 145 and 210 cm^{-1} of powdered **1** (which have diffuse counterparts in the IR spectrum) appear only in the Raman spectrum of the pe/pe combination (see Figure 6), indicating that they correspond to skeletal modes of E′ or innerligand vibrations of e_2 symmetry. As the latter move between 104 and 237 cm^{-1} and 173−270 cm^{-1}, respectively (see Table 5), no definite assignments can be given. The polarization properties of the diffuse band at about 330 cm^{-1} are difficult to recognize. It can be observed weakly in the Raman spectrum of the pe/pe, and perhaps additionally in the pa/pa combination (see Figure 6).

(52) Bencze, É.; Mink, J.; Németh, C.; Herrmann, W. A.; Lokshin, B. V.; Kühn, F. E. *J. Organomet. Chem.* **2002**, *642*, 246.

At 94 cm^{-1}, a weak signal appears in the FIR spectrum and very strong bands at 99 and 93 cm^{-1} in the pa/pe and pe/pe combinations, respectively. At the present stage these findings allow no further assignments.

4. Conclusions and Outlook

$SmCp^*_3$ is one of the rare organometallics of f elements which exhibits f-f transitions in the FIR/MIR range. Additionally, electronic Raman transitions could be observed even at room temperature. Low temperature FIR/MIR and electronic Raman spectra, where f-f and electronic Raman transitions are noticeably enforced, compared to vibrational signals, would be highly desirable, to detect additional CF levels.

The fit of the CF energies of **1** leads to free ion and CF parameters, the interpretation of which demonstrates that **1** is the most covalent Sm^{III} compound known to date (considering only the f electrons) and that the Sm^{3+} central ion of **1** experiences the third largest CF strength ever encountered in samarium(III) chemistry.

A non-relativistic calculation (Xα-SW approximation) on ψ trigonal planar model complex $Sm(\eta^5\text{-}Cp)_3$ overestimates the total splitting of f orbitals by a factor of 1.5 (compared with the experimentally based non-relativistic one).

By applying the selection rules (of local D_{3h} symmetry for the Sm^{3+} central ion and local C_{5v} symmetry for the Cp* ligands) to the observed FIR (pellets) and polarized Raman spectra of oriented $SmCp^*_3$ single crystals, the irreducible representations of some skeletal vibrations could be determined. Several attempts to organize polarized FIR measurements of oriented single crystals failed.

In contrast to dark brown single crystals of $SmCp^*_3$, the yellow ones of $LaCp^*_3$ allow the application of the exciting line at 532 nm of our Raman apparatus. For this reason, better resolved Raman spectra are expected and the recording of innerligand vibrations with higher wavenumbers will be possible. The interpretation of the observed FIR and polarized Raman spectra of $LaCp^*_3$ will be accompanied by calculations with the program RIDFT (TURBOMOLE). However, the lower number of vibrating atoms of the sandwich complex $RuCp^*_2$ would reduce both the experimental assignment and the computational problems, thus suggesting to tackle this compound prior to $LaCp^*_3$.

Note Added after ASAP Publication. The version of this paper published on October 16, 2009, contained the wrong Figure 3. The corrected version was published on October 22, 2009.

Acknowledgment. The financial support of the "Deutsche Forschungsgemeinschaft" and the "U.S. National Science Foundation" is gratefully acknowledged.